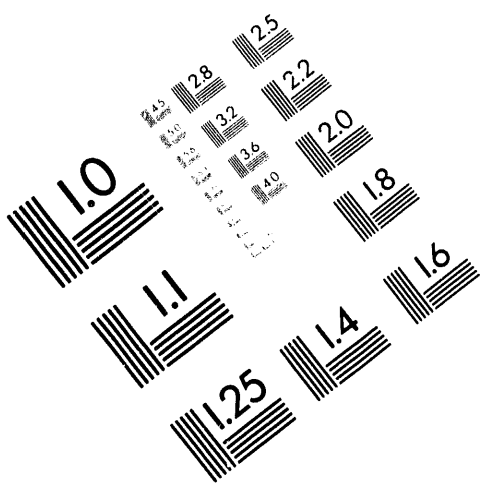

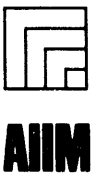

Association for Information and Image Management

1100 Wayne Avenue, Suite 1100
Silver Spring, Maryland 20910

301/587-8202

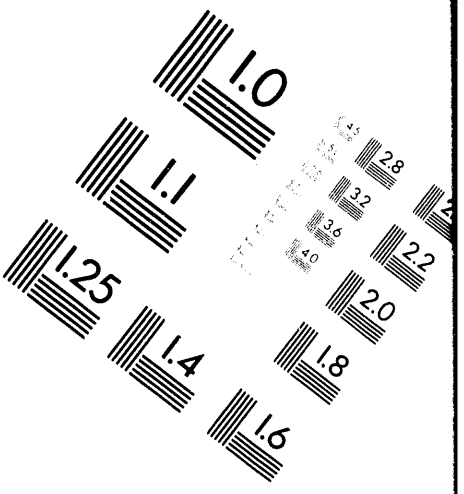

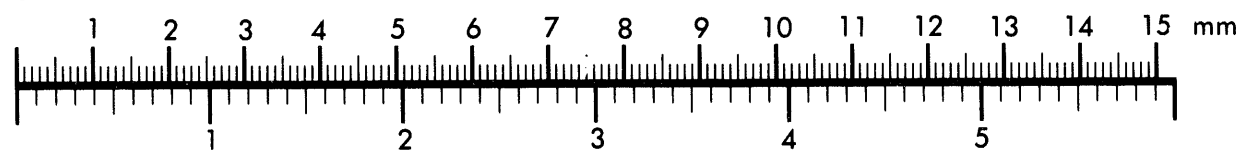

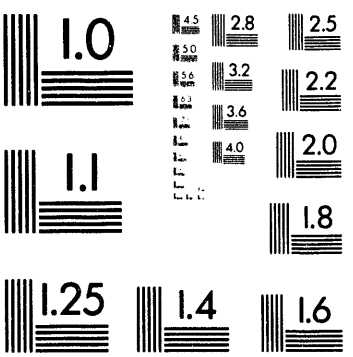

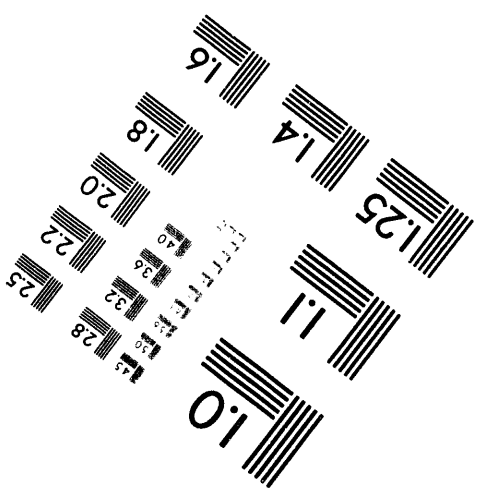

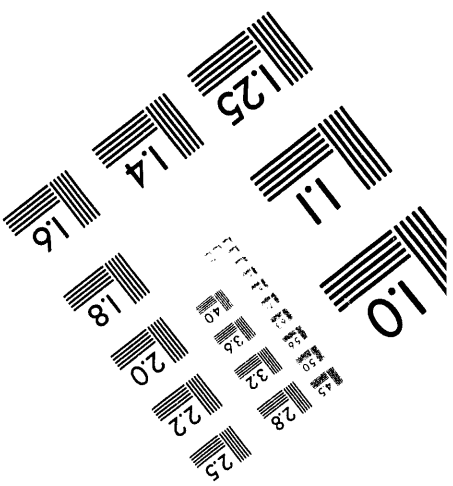

MANUFACTURED TO AIIM STANDARDS
BY APPLIED IMAGE, INC.

1 of 1

DOE/ER/40270--53
CONF-9305241--5
MKPH-T-93-11

Invited talk presented at the 6th Workshop on Perspectives in Nuclear Physics
at Intermediate Energies, Trieste, 1993

POLARIZATION OBSERVABLES IN PION PHOTOPRODUCTION ON LIGHT NUCLEI [§]

L. Tiator[1], *S.S. Kamalov*[2], *and C. Bennhold*[3]

[1] Institut für Kernphysik, Universität Mainz, 55099 Mainz, Germany
[2] Laboratory of Theoretical Physics, JINR Dubna, Russia
[3] Department of Physics, Center of Nuclear Studies, The George Washington University, Washington, D.C., 20052, USA

Abstract

Single polarization observables Σ, P and T are investigated for the nucleon (p, n) and the trinucleon (^3He, ^3H). The threshold E_{0+} and the resonance M_{1+} and E_{1+} multipoles are particularly studied. For the reaction $^3\mathrm{He}(\gamma,\pi^+)^3\mathrm{H}$ a recently developed nonlocal coupled-channel approach is presented that employs three-body Faddeev amplitudes and incorporates two-step processes such as $^3\mathrm{He}(\gamma,\pi^\circ)^3\mathrm{He}(\pi^\circ,\pi^+)^3\mathrm{H}$. Enhancement effects of the contributions from small components of the ^{3}He wave function as well as from the Δ resonance E2 transition to the polarization observables have been found.

1. Introduction

Polarization observables have the promise of opening a new field in the electromagnetic production of pions from nucleons and nuclear targets. Since many of these observables contain interference terms, small but important amplitudes can be investigated in a unique way. The new generation of 100% duty factor, high intensity electron accelerators will have the potential to provide high quality polarized electron and photon beams as well as the capabilities of performing coincidence experiments which could not be carried out until now. Such measurements will be forthcoming at the accelerators in Mainz (MAMI), NIKHEF-K (AmPS), Saskatoon and MIT/Bates.

In the elementary reaction on the nucleon there are two energy regions where polarization degrees of freedom are heavily needed to clearify important questions of the underlying theoretical descriptions of pion photoproduction. These are the threshold region, where the validity of the Low Energy Theorems is still not finally clearified and the resonance region, where the small E2 quadrupole excitation of the Δ resonance cannot be accurately determined from present data.

Pion photoproduction off ^{3}He is an ideal testing ground to investigate the interaction of pions and photons with nuclei and search for possible modifications of delta properties in the nuclear medium. Nuclear structure uncertainties in the trinucleon wave function are under control since correlated three-body amplitudes can be obtained [1, 2, 3] by solving the Faddeev equations with realistic nucleon-nucleon potentials.

In this paper we first study the threshold γ,π^0 on the proton and show the importance of beam asymmetry and target polarization in order to get information on the small p-wave multipoles E_{1+} and M_{1-} and the imaginary part of the E_{0+} multipole.

[§] This work was supported by the Deutsche Forschungsgemeinschaft (SFB201) and the U.S. DOE grant DE-FG05-86-ER40270

In the resonance region we demonstrate the small effect of the E2(Δ) which is mostly pronounced in the beam asymmetry. In the main part of this work we then compare the polarization observables on the nucleon with the observables on the trinucleon. The calculations are performed within a recently developed coupled-channel framework [4] that can consistently describe π^+ and coherent π° photoproduction as well as elastic and charge-exchange pion scattering on ^{3}He. After properly including pion final state interaction (FSI) with the important two-step process $^3\mathrm{He}(\gamma,\pi^\circ)^3\mathrm{He}(\pi^\circ,\pi^+)^3\mathrm{H}$ a good description of the $^3\mathrm{He}(\gamma,\pi^+)^3\mathrm{H}$ data for the differential cross sections has been achieved over a wide range of photon energies and nuclear momentum transfers. Here we will focus less on differential cross sections but rather on the sensitivity of P, T and Σ to details in the trinucleon wave function and in the elementary production operator.

2. Polarization Observables

For spin 1/2 particles (p, n, ^3He, ...) the differential cross section for reactions induced by real photons including polarization degrees of freedom is given in the c.m. system by

$$\begin{aligned}\frac{d\sigma}{d\Omega} &= \frac{k}{q}\{(R_T + P_n R_T^n) \\ &+\Pi_T[(R_{TT} + P_n R_{TT}^n)\cos 2\varphi - (P_l R_{TT}^l + P_t R_T^t)\sin 2\varphi] \\ &+\Pi_C(P_l R_{TT'}^l + P_t R_{TT'}^t)\},\end{aligned} \tag{1}$$

where Π_T is the degree of linear polarization of the photon and φ the angle of the polarization vector relative to the reaction plane, and Π_C is the degree of circular polarization. For example, for completely linearly polarized photons and polarization vector normal to the production plane, Π_T=1, $\varphi=\pi/2$ and Π_C=0, while right (left)-circularly polarized photons have Π_T=0 and Π_C=+1(-1).

In addition to the photon polarization, there appear the projections of the target/recoil spin unto the axes $\{\hat{n},\hat{l},\hat{t}\}$, where $\hat{n} = \hat{q}\times\hat{k}/\sin\Theta_\pi$ (normal to the reaction plane), $\hat{l}$ (along the proton momentum) and $\hat{t} = \hat{n}\times\hat{l}$. For example, $P_n = \hat{s}_R\cdot\hat{n}$ is the projection of the spin vector (in the particle rest frame!) unto the axis normal to the production plane. Throughout this paper we use q (k) for photon (pion) momenta.

The response functions R_T, R_{TT}, *etc.* are bilinear combinations of the hadronic current J and are defined in the same way as in an electroproduction experiment, where in addition to the transverse components also longitudinal components appear. Details and multipole expansions of the response functions can be found in ref [5].

In experiments with polarization degrees of freedom it is common to define the following observables:

(i) the polarized photon asymmetry (beam asymmetry)

$$\Sigma(\Theta) = -R_{TT}/R_T \tag{2}$$

(ii) the polarized target asymmetry

$$T(\Theta) = R_T(n_i)/R_T = -R_{TT}(n_f)/R_T \tag{3}$$

(iii) the recoil polarization

$$P(\Theta) = R_T(n_f)/R_T = -R_{TT}(n_i)/R_T, \tag{4}$$

where n_i and n_f refers to the polarization of the nucleon (nucleus) in the initial and final state and Θ is the pion angle in the c.m. system.

In addition there are four observables for polarization of beam and target, four of beam and recoil and four of target and recoil polarization. [6, 7] As shown by Barker et al [6] a complete experiment requires besides the differential cross section and the three single polarization observables five double polarization observables, provided that no four of them come from the same set (beam-target, beam-recoil and target-recoil).

Alternatively we can define the single polarization observables in the following way

$$\Sigma = \frac{d\sigma/d\Omega^{\perp} - d\sigma/d\Omega^{\parallel}}{d\sigma/d\Omega^{\perp} + d\sigma/d\Omega^{\parallel}} \tag{5}$$

$$T = \frac{d\sigma/d\Omega^{(+)} - d\sigma/d\Omega^{(-)}}{d\sigma/d\Omega^{(+)} + d\sigma/d\Omega^{(-)}} \tag{6}$$

$$P = \frac{d\sigma/d\Omega^{(+)} - d\sigma/d\Omega^{(-)}}{d\sigma/d\Omega^{(+)} + d\sigma/d\Omega^{(-)}} \tag{7}$$

where $+(-)$ refers to the initial or final nucleus polarized parallel (antiparallel) to the $\hat{n}$-axis, and $\perp$ ($\parallel$) refers to a photon linearly polarized perpendicular (parallel) to the production plane.

3. Pion Photoproduction on the Nucleon

As a first application for polarized observables we want to discuss the threshold pion photoproduction on the nucleon. Expressed in s- and p-wave multipoles and neglecting terms that are quadratic in the small p-wave multipoles E_{1+} and M_{1-}, the differential cross section is given by

$$\frac{d\sigma}{d\Omega} = \frac{k}{q}(A + B\cos\Theta + C\cos^2\Theta) \tag{8}$$

$$A = |E_{0+}|^2 + \frac{5}{2}|M_{1+}|^2 - Re\{M_{1+}^*(3E_{1+} - M_{1-})\}$$

$$B = 2Re\{E_{0+}^*(M_{1+} + 3E_{1+} - M_{1-})\}$$

$$C = -\frac{3}{2}|M_{1+}|^2 + 3Re\{M_{1+}^*(3E_{1+} - M_{1-})\}.$$

In Fig. 1 we show the threshold amplitudes for $p(\gamma,\pi^0)p$ determined from the cross section data of the Mainz experiment, Beck et al [8].The error band for the M1 amplitude and the five solid points are from the analysis of Drechsel and Tiator [5]. The open circles show the E_{0+} multipole obtained from the total cross sections, when the p-wave contributions [5] are subtracted.

Close to the γ,π^0 threshold the data approaches the prediction of the Low Energy Theorems, around the γ,π^+ threshold, however, the amplitude is consistent with zero. In Fig. 1b we also show the calculations of Bernard et al [9, 10, 11] in chiral perturbation theory. While a consistent 1-loop calculation [9] assuming isospin symmetry gives a threshold value of $-1.33 \cdot 10^{-3}/m_{\pi^+}$, an approximate treatment of isospin breaking due to different pion and nucleon masses also calculated in 1-loop gives a cusp effect similar to K-matrix calculations and a shape closer to the data [10].

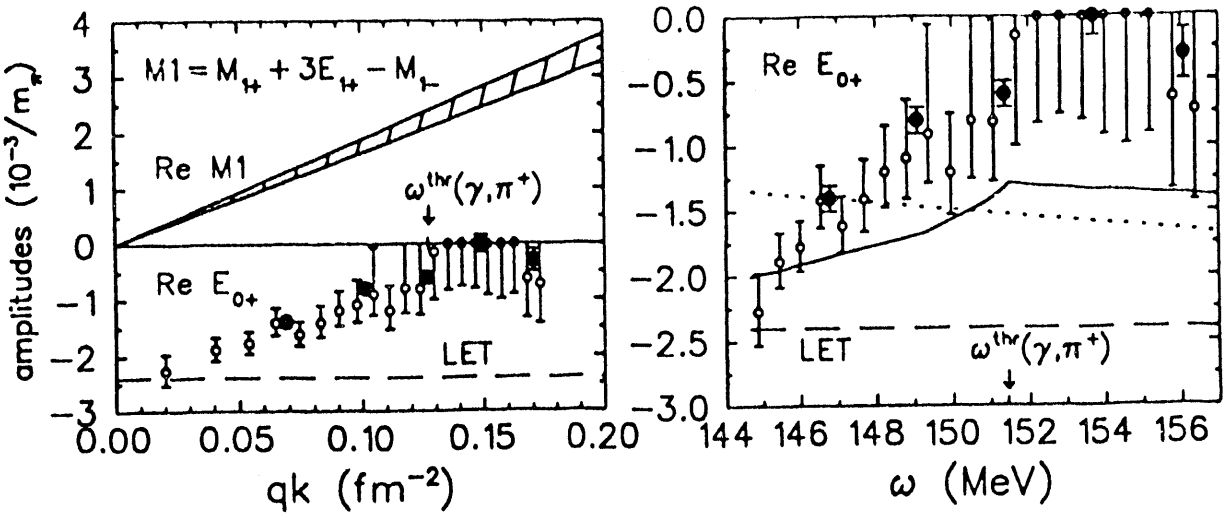

Fig. 1: Threshold s- and p-wave multipoles for $p(\gamma,\pi^0)p$. The p-wave error band and the full dots show the combined analysis of differential and total cross sections [5] obtained from the data of Beck et al [8]. The open circles show our analysis obtained from the total cross sections by subtracting the p-wave amplitudes of ref [5]. The error bars give the total correlated errors from the cross sections and from the determination of the p-wave multipoles. The dotted and full lines show the results of chiral perturbation theory [9, 10] for isospin symmetry and isospin breaking due to the physical pion and nucleon masses respectively.

While the differential cross section is very sensitive to the asymmetry parameter B in equ. (8), and therefore to the real parts of E_{0+} and the p-wave combination M1, a complete analysis of the threshold region with separation of the individual p-wave multipoles and the imaginary part of the s-wave can only be obtained with polarization observables. In the same approximation as in equ. (8) the three single polarization observables are given by

$$\Sigma = \frac{3k\sin^2\Theta}{2q d\sigma/d\Omega}(|M_{1+}|^2 + 2Re\{M_{1+}^*(E_{1+}+M_{1-})\} \quad (9)$$

$$T = \frac{3k\sin\Theta}{q d\sigma/d\Omega} Im\{E_{0+}^*(E_{1+}-M_{1+}) - cos\Theta M_{1+}^*(4E_{1+}+M_{1-}\} \quad (10)$$

$$P = -\frac{k\sin\Theta}{q d\sigma/d\Omega} Im\{E_{0+}^*(3E_{1+}+M_{1+}+2M_{1-}) + 3cos\Theta M_{1+}^* M_{1-}\}. \quad (11)$$

The target and recoil polarizations are very sensitive to the imaginary part of the s-wave amplitude and the beam asymmetry gives together with the differential cross section another linear independent measurement of the small p-wave multipoles. In Fig. 2 we demonstrate these effects with a calculation done by Davidson [12]. The target asymmetry is directly proportional to ImE_{0+} and shows a very steep rise at the charged pion threshold. As also pointed out by Bernstein [13], a measurement of this quantity provides the only possibility to measure directly the πN scattering lengths which is a very sensitive test to chiral dynamics. In the region below the charged pion threshold there is even a possibility to observe the isoscalar scattering length for $\pi^0 p$ scattering. However due to the smallness of this amplitude, the target asymmetry will be around a hundred times smaller than in the region where the isovector amplitude dominates. From the small isoscalar scattering length not even the sign is known, the calculation presented

here assumes a negative sign and a value of $a(\pi^0 p) = -.005/m_\pi$. In Fig. 2b we show the possibility to disentangle the small p-wave multipoles, all three curves would be totally consistent with the differential cross section data.

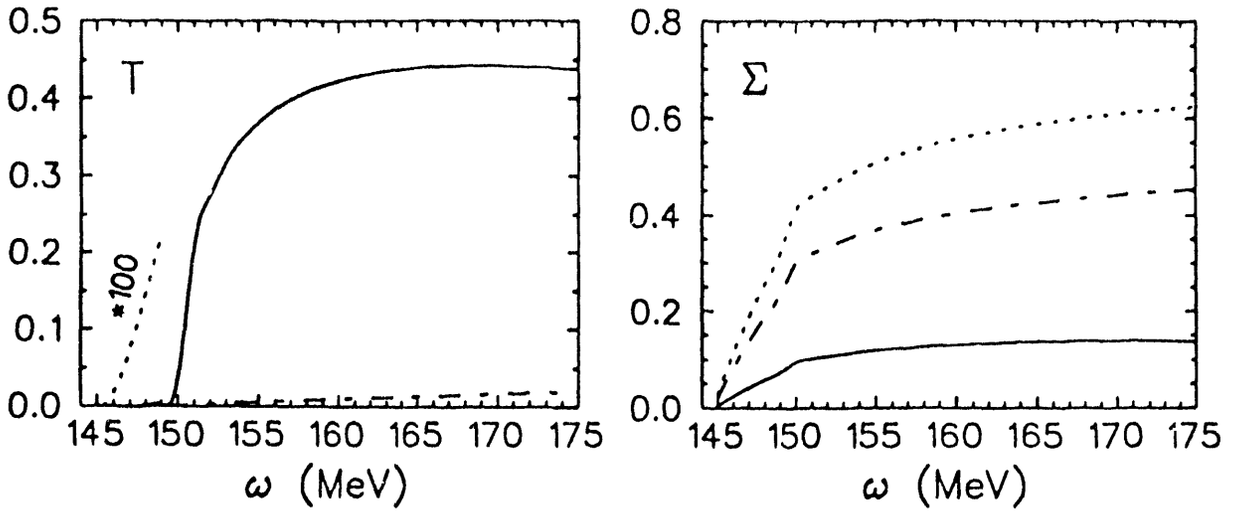

Fig. 2: Target asymmetry (T) and photon asymmetry (Σ) for threshold $p(\gamma,\pi^0)p$ at $\Theta_{c.m.} = 90°$. In a) the solid line shows the full calculation and the dash-dotted line the situation for ImE_{0+}=0. The dotted curve is a magnification of the full line by a factor of 100 in the region between the neutral and the charged pion thresholds. In b) the full, dash-dotted and dotted lines are obtained for (E_{1+}, M_{1-}) = (-0.5, -2.3), (0, -0.8) and (0.3, 0) respectively. Note that all three sets give $3E_{1+}$-M_{1-}=0.8 in agreement with the analysis shown in Fig. 1. (All p-wave multipoles are given in units of $qk \cdot 10^{-3}/m_{\pi^+}^3$)

Finally in Fig. 3 we show the beam asymmetry and the recoil polarization for the reaction $p(\gamma,\pi^+)n$ in the Δ region. Both observables are dominated by the Δ excitation that is mainly M1 transition. While the recoil polarization and similarly the target asymmetry are entirely determined by the resonance contribution and give zero result in Born approximation, the beam asymmetry shows a nonnegligible background which is mainly coming from the pion pole term. In π^0 photoproduction, where this term vanishes, also the beam asymmetry is almost entirely given by the resonance contribution. Assuming a 5% E2 contribution to the Δ excitation, which was parametrized by Laget [14] and used in this calculation and in the calculations on ^{3}He below, we find almost no effect in the recoil or target polarizations and a small but sizable effect in the beam asymmetry. This sensitivity will be used in a Mainz experiment that has been proposed by Beck et al [15] and that is measuring the photon asymmetry on the proton for neutral and charged pions in order to separate the isospin 1/2 and 3/2 channels.

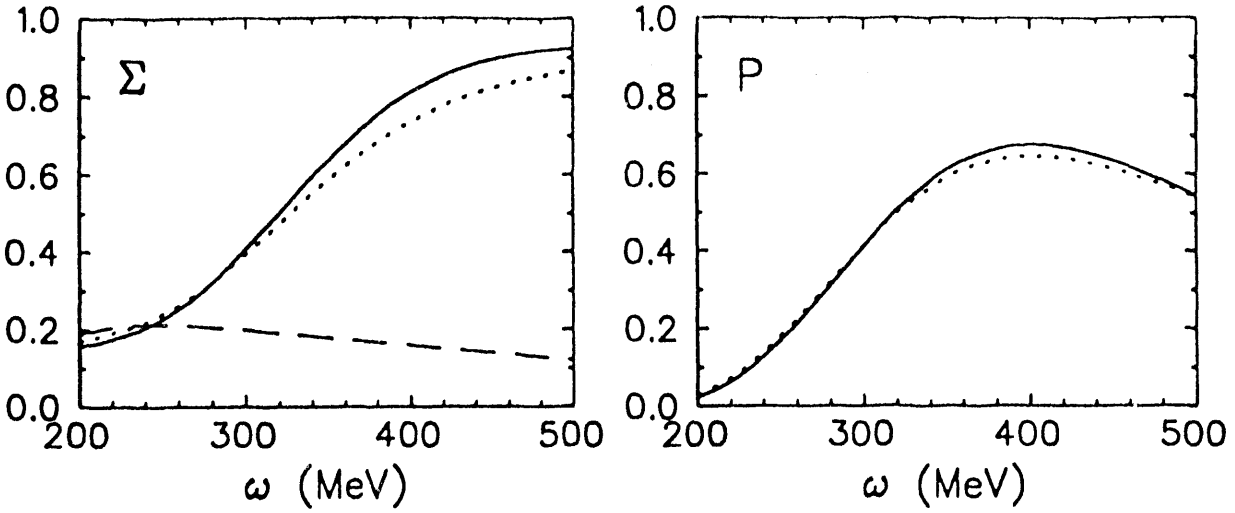

Fig. 3: Photon asymmetry (Σ) and recoil polarization (P) for $p(\gamma,\pi^+)n$ at $\Theta_{c.m.} = 90°$ in the Δ region. The solid line shows the full calculation and the dash-dotted line the situation with $E_{1+}(\Delta)$=0. The dashed curve gives the contribution of the Born terms alone and vanishes for the recoil polarization. The calculations are from [16].

4. Coupled-channels framework for $^3\mathrm{He}(\gamma,\pi^+)^3\mathrm{H}$

In momentum space the nuclear photoproduction amplitude can be written as

$$F_{\pi\gamma}(k,q) = V_{\pi\gamma}(k,q) - \frac{a}{(2\pi)^2}\sum_{\pi'}\int \frac{d^3k'}{M(k')}\frac{F_{\pi\pi'}(k,k')V_{\pi'\gamma}(k',k)}{E(k)-E(k')+i\epsilon}\ , \tag{12}$$

where q (k) is the photon (pion) momentum, and $\pi = 0,\pm1$ is the pion charge in the intermediate state. The total pion-nuclear energy is denoted by $E(k) = E_\pi(k) + E_A(k)$, the reduced mass is given by $M(k) = E_\pi(k)E_A(k)/E(k)$ and $a = (A-1)/A = 2/3$. In the framework of the impulse approximation $V_{\pi\gamma}$ is expressed in terms of the free pion-nucleon photoproduction t-matrix:

$$V_{\pi\gamma}(k,q) = -\frac{\sqrt{M(q)M(k)}}{2\pi} < \pi(k), f \mid \sum_{j=1}^{A}\hat{t}_{\gamma N}(j) \mid i,\gamma(q) >, \tag{13}$$

where $\mid i >$ and $\mid f >$ denote the nuclear initial and final states, respectively, and j refers to the individual target nucleons. Detailed information about the way of construction of $V_{\pi\gamma}(k,q)$ is given in our previous paper [4]. Note only that for $\hat{t}_{\gamma N}$ we shall use the modern unitary version of the Blomqvist-Laget amplitude [14], which describes the real and imaginary parts not only for the resonance magnetic M_{1+} but also for the resonance E_{1+} multipole.

Using the KMT version of multiple scattering theory [17] the pion scattering amplitude $F_{\pi'\pi}$ is constructed as a solution of the Lippmann-Schwinger equation

$$F_{\pi'\pi}(k',k) = V_{\pi'\pi}(k',k) - \frac{a}{(2\pi)^2}\sum_{\pi''}\int \frac{d^3k''}{M(k'')}\frac{V_{\pi'\pi''}(k',k'')F_{\pi''\pi}(k'',k)}{E(k)-E(k'')+i\epsilon}\ . \tag{14}$$

Here the pion-nuclear interaction is described by the first-order potential $V_{\pi'\pi}$ which is related to the free πN scattering t-matrix [18]

For the description of ^{3}He and ^{3}H we use the trinucleon wave function in momentum space, expanded in the orbital angular momentum, spin, and isospin space as

$$\Psi(P,p) = \sum_\alpha \phi_\alpha(P,p) \mid (L\ell)\mathscr{L}, \left(S\tfrac{1}{2}\right)\mathscr{S}, \tfrac{1}{2}M > \mid \left(T\tfrac{1}{2}\right)\tfrac{1}{2}N > \qquad (15)$$

where $\phi_\alpha(P,p)$ are the numerical solutions of the Faddeev equations [1]. The individual partial waves are denoted by $\alpha \equiv \{L\,\ell\,\mathscr{L}\,S\,\mathscr{S}\,T\}$, where L, S, and T are the total orbital momentum, spin and isospin of the pair (2,3) (L is correlated with momentum P), while ℓ is the orbital momentum of particle (1) which is correlated with linear momentum p. In our model we include 11 partial waves listed in table 1. The dominant part of the wave function, about 90%, consists of S-state amplitudes while the D-state probabilities combine to around 8%.

Table 1

α	L	ℓ	$\mathscr{L}$	S	$\mathscr{S}$	T	$P(\%)$
1	0	0	0	1	1/2	0	45.2
2	0	0	0	0	1/2	1	44.5
3	2	2	0	1	1/2	0	0.5
4	2	2	0	0	1/2	1	0.9
5	1	1	0	0	1/2	0	0.4
6	1	1	0	1	1/2	1	0.4
7	2	0	2	1	3/2	0	3.1
8	0	2	2	1	3/2	0	1.0
9	1	1	2	1	3/2	1	2.5
10	3	1	2	1	3/2	1	0.4
11	1	3	2	1	3/2	1	1.0

5. PWIA analysis

To qualitatively understand the results which will be given below we begin our investigation with a very simple model using harmonic oscillator S-shell nuclear wave functions and excluding pion rescattering (the second term in eq. (12)). In this case we obtain simple relations between the observables for $^3\mathrm{He}(\gamma,\pi^+)^3\mathrm{H}$ and the elementary process $p(\gamma,\pi^+)n$

$$\Sigma(^3\mathrm{He}) = \Sigma(p), \qquad T(^3\mathrm{He}) = -P(p) \quad \text{and} \quad P(^3\mathrm{He}) = -T(p), \qquad (16)$$

provided the Lorentz transformation from the πN c.m. to the π^3He c.m. system has been taken into account. The minus sign in eq. (16) is due to an opposite sign between spin-flip and non spin-flip matrix elements in $^3\mathrm{He}(\gamma,\pi^+)^3\mathrm{H}$ compared to the free process $p(\gamma,\pi^+)n$. This is a result of the Pauli principle forbidding non spin-flip transitions on that proton in ^{3}He whose spin is aligned with that of the neutron.

From the relations (16) one may conclude that it would be difficult to extract new information from the study of polarization observables in ^{3}He. However, this is true only for simple models in which the contributions from D-wave components of the ^{3}He wave functions have been neglected. In realistic models these relatively small components can produce drastic effects on polarization observables, as we shall see below.

For illustration let us consider the photon asymmetry Σ. If we keep only the largest S-state components ($\alpha = 1$ and $\alpha = 2$ in the notation of table 1) in the three-body wave function (15) and the lowest pion-nucleon s- and p-waves in the elementary amplitude $t_{\gamma N}$, then the photon asymmetry can be expressed using the elementary multipoles $E_{l\pm}$ and $M_{l\pm}$ in the following way

$$\Sigma_S = \frac{\sin^2\Theta}{d\sigma_A/d\Omega}\left[C^2(Q) \mid 2M_{1+} + M_{1-} \mid^2 - \frac{1}{3}S_M^2(Q) \mid f_{EM} \mid^2\right], \qquad (17)$$

where

$$f_{EM} = 3E_{1+} - M_{1+} + M_{1-}, \qquad (18)$$

$C(Q)$ and S_M are non spin-flip and spin-flip nuclear formfactors, respectively. The explicit expressions for them are presented in ref [4]. Note that in the harmonic oscillator S-shell model the following simple relation between the spin-flip and non spin-flip formfactors holds

$$S_M(Q) = -\sqrt{3}C(Q) \qquad (19)$$

Realistic trinucleon wave functions modify this relation only slightly as long as only S-waves are considered. Substituting (19) in expression (17) leads to

$$\Sigma_S = \frac{k}{q}\frac{3\sin^2\Theta}{d\sigma_N/d\Omega}\left\{\frac{1}{2} \mid M_{1+} \mid^2 - \frac{3}{2} \mid E_{1+} \mid^2 + Re\left[E_{1+}^*(M_{1+} - M_{1-}) + M_{1+}^* M_{1-}\right]\right\} \qquad (20)$$

The differential cross section expression for the process on ^{3}He in such a simple model is the same as for the process on the proton, except for some common multiplicative factor which is proportional to $C(Q)$ and which cancels in the expressions for the polarization observables (see equ. (9)).

If we take into account all 11 components of the trinucleon wave function additional contributions to the photon asymmetry arise. The most important one is due to an interference between S- and D-state components. Explicitly, the corresponding additional contribution at $\Theta_{c.m.} = 90^0$ can be expressed in terms of the elementary multipoles in the following way

$$\Sigma_{SD}(90^0) \sim S_M(Q)\, D_M(Q)\left[\mathrm{Re}E_{0+}f_{EM}^* - \frac{q}{2k} \mid E_{0+} \mid^2 - \frac{4q^2+k^2}{2kq} \mid f_{EM} \mid^2\right], \qquad (21)$$

Comparing expressions (21) and (20) it becomes apparent that we obtain an enhancement of the D-state component contributions (the correspondin spin-flip formfactor is D_M) due to the large Kroll-Ruderman E_{0+} multipole which is absent for a pure S-wave function, as well as for the photon asymmetry of the elementary process.

Another interesting effect has to do with the contribution of the E_{1+} amplitude, which is of a particular interest because its resonance part describes the E2 transition in the

$\gamma N\Delta$ vertex. It is well known that the electromagnetic excitation of the Δ is mainly magnetic dipole M1, leading to the multipole amplitude M_{1+}, since it proceeds through a quark spin flip. However, its quadrupole component, showing up in the E_{1+} amplitude, is of great interest since it is sensitive to the tensor force in the quark-quark interaction and gives a measure of the deformation of the delta and subsequently also of the nucleon.

As we can see from eq. (21), the interference of the E_{0+} and E_{1+} multipoles which arises in the photon asymmetry due only to the D-state component drastically increases the sensitivity of the photon asymmetry to this E2 transition, in contrast to the free proton case. Note that in the differential cross section such an enhancement effect is much smaller due to the large background produced by the E_{0+} and M_{1+} multipoles.

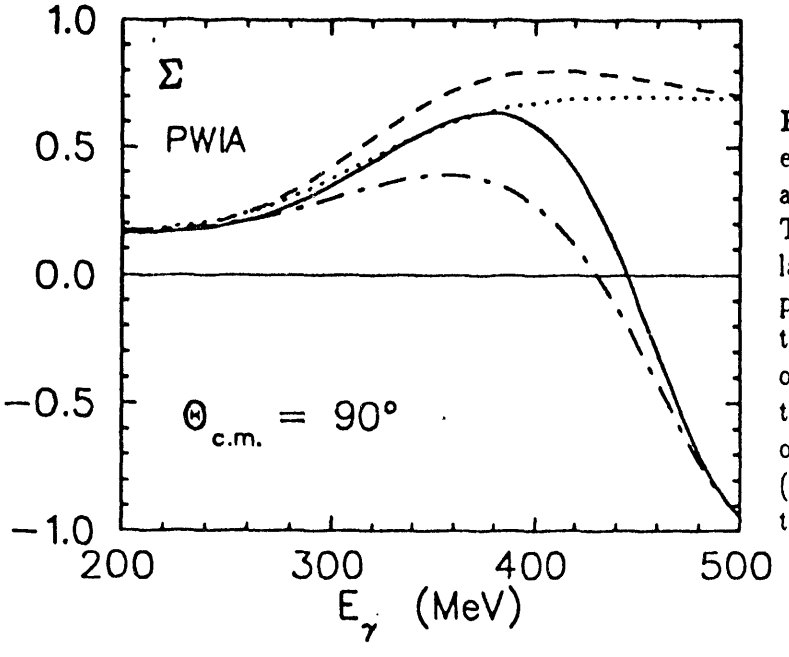

Fig. 4: Plane wave results for the energy dependence of the photon (Σ) asymmetries at pion c.m. angle 90°. The solid (dashed) curves are calculations with (without) D-state components of the three-body wave function [1] and with the full production operator [14]. The dash-dotted (dotted) curves are calculations without the $E_{1+}(\Delta)$ multipole and with (without) D-state components of the three-body wave function.

The effects found above are illustrated in Fig. 1. Here we compare our PWIA calculations at $\Theta_{c.m.} = 90°$ obtained with the full trinucleon wave function and one that contains only S-components ($\alpha = 1$ and $\alpha = 2$). With increasing photon energy the contribution from D-state components of ^{3}He becomes larger and at $E_\gamma = 450$ MeV the photon asymmetry changes sign. We found that this can be attributed to the configuration $\alpha = 8$ (see table 1) which has only 1% probability but entirely determines the isovector $D_M(Q)$ formfactor. This can easily be understood in PWIA, where the interaction takes place only on one of the three nucleons therefore leaving the pair unaffected, i.e. $L = L', S = S'$ and $T = T'$. From table 1 it then becomes clear that the only interference terms between S- and D-state components will be $(\alpha, \alpha') = (1, 8)$ and (8,1).

Fig. 4 also compares PWIA calculations using the full elementary amplitude with one that does not contain the E2(Δ) transition in the $\gamma N\Delta$ vertex. From the results depicted here it follows that the sensitivity of the photon asymmetry to the E2(Δ) transition is enhanced when using the full wave function compared to using only their S-state components. Thus D-wave configurations enhance the role of the E_{1+} multipole as expected and, consequently, the role of the E2(Δ) transition.

The target asymmetry T is less sensitive to the details of nuclear structure and the E_{1+} multipole contribution. This is due to the dominance of the E_{0+} and M_{1+} multipoles both in the numerator and denominator of eq. (10). Our calculations lead to the same

conclusion for the recoil asymmetry P.

In the next section we present the results of our full calculation which includes a proper treatment of pion rescattering. Even though these contributions are important they do not significantly change the effects found here.

6. Coupled-channels calculations

To take into account pion rescattering contributions (FSI) we will use the coupled-channels method developed in our previous work [4]. It is based on the numerical solution of the system of equations (12) and (14) with three-body Faddeev wave functions and gives an excellent description of pion elastic and pion single charge exchange (SCE) reactions at low pion energies and in the Δ resonance region.

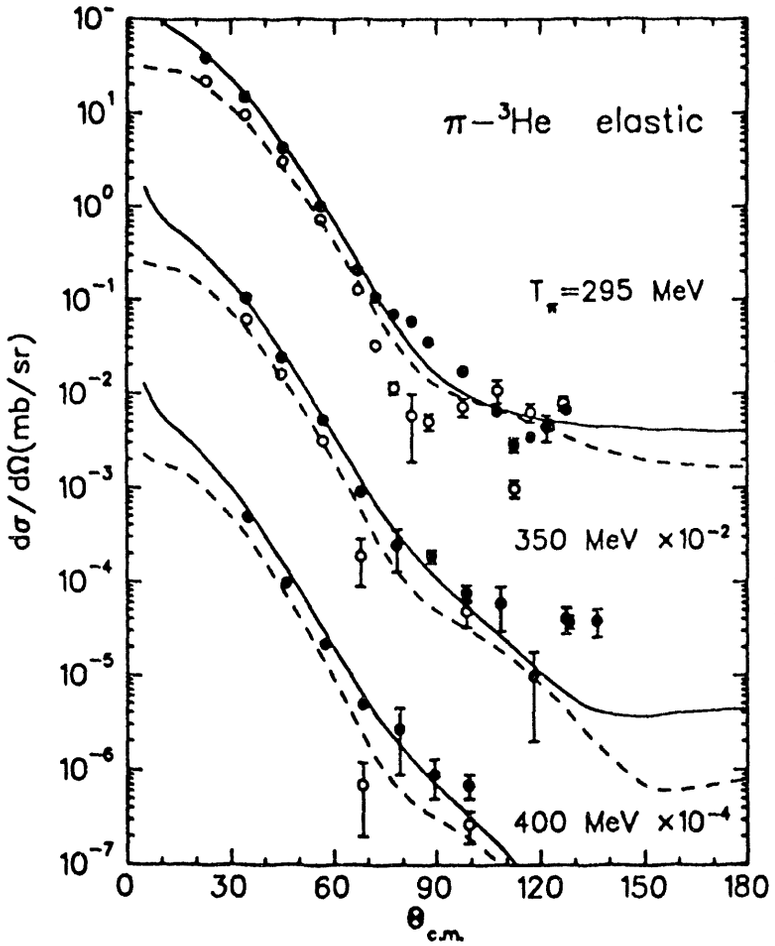

Fig. 5: Differential cross sections for π^+ (solid curves) and π^- (dashed curves) elastic scattering on ^{3}He at pion kinetic energies T_π = 295, 350 and 400 MeV calculated with the full three-body wave function [1]. Experimental data for $\pi^+(\bullet)$ and $\pi^-(\circ)$ are from ref [19] for 295 MeV and ref [20] for 350 and 400 MeV.

Fig. 5 presents the results for $\pi^\pm$ elastic scattering at higher energies which demonstrates that in the region $T_\pi = 300 - 400$ MeV (corresponding to photon energies $E_\gamma = 440 - 540$ MeV) we can also reach good agreement with the experimental data from refs [19, 20]

Note that the good agreement with the data both for π^+ and π^- elastic scattering at forward direction gives us confidence in the accuracy of the isovector part of the pion-nuclear interaction which is responsible for the pion SCE reaction. The small disagreement at larger angles (were $d\sigma/d\Omega$ is more than 10^{-3} times smaller) is not too serious since only angle-integrated characteristics of the (π', π) reaction enter into the pion photoproduction amplitude.

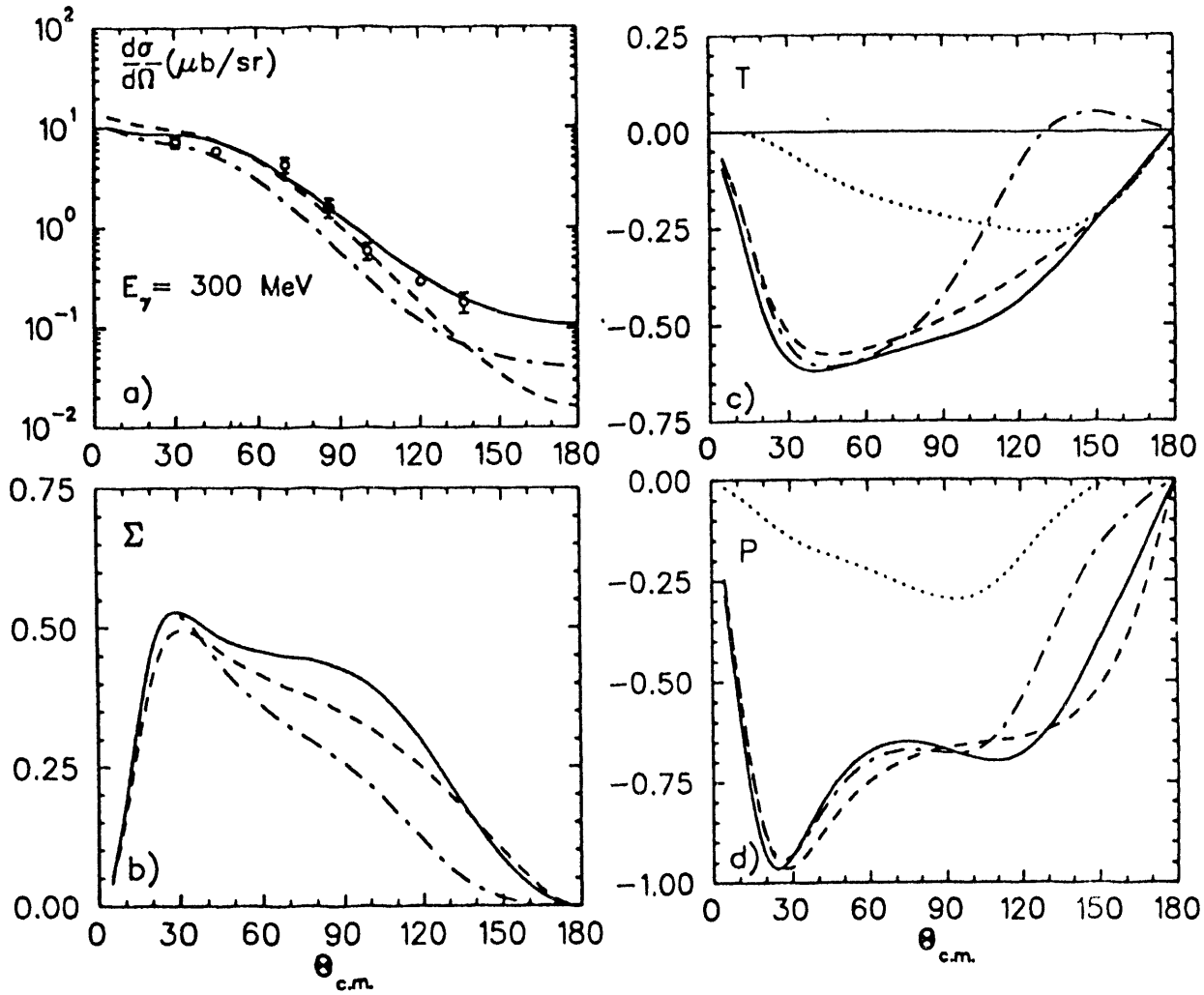

Fig. 6: Angular distributions (a) and polarization observables (b-d) at E_γ=300 MeV calculated with the full three-body wave function and the full production operator. Solid, dash-dotted and dashed curves are the results obtained in the coupled-channels approach that includes two-step processes, in DWIA and PWIA, respectively. Experimental data are from ref [21](o) and ref [22](•). The dotted curves are the results obtained by the coupled-channels method with the full three-body wave function but only with Born terms in the production operator.

Returning to pion photoproduction we first discuss the angular distribution of the cross section and polarization observables at a fixed photon energy to shed more light on pion rescattering effects at different pion angles. In Fig. 6 we compare our results obtained with the full Faddeev wave function using PWIA, standard DWIA which does not include two-step processes, and the coupled-channels method which incorporates the contributions from the ^{3}He$(\gamma,\pi^0)^3$He$(\pi^0,\pi^+)^3$H channel. This comparison shows that, even though pion rescattering is important to reproduce the differential cross section, there is very little change in the polarization observables in the forward direction ($\Theta_{c.m.} < 50°$). This can be understood in the framework of the Eikonal approach, where FSI at small angles can be described with a simple distortion factor, that drops out in the numerators and denominators of eqs. (5-7). However, at larger angles this simple approach is not valid any more and, therefore, pion rescattering contributions to the polarization observables become more important. Note that the complete treatment of FSI provides a much improved description of the Saclay measurements for the differential cross section at $E_\gamma =$ 300 MeV [21].

The influence of pion final state interaction on the observables T and P can also be seen by removing the Δ contribution from the production operator. In this case the amplitudes become real and, consequently, in PWIA calculations we obtain zero for these observables because they are proportional to the imaginary part of the photoproduction amplitude. Our coupled-channels calculations with only Born terms in the elementary operator (dotted curves) yield rather small results for T and P at forward angles where the influence of FSI is very small. However, at larger angles T and P computed with Born terms only become larger due to increasing FSI effects.

In accordance with our previous results [4], the largest contribution of the two-step process $(\gamma,\pi^0)(\pi^0,\pi^+)$ comes from the coherent non spin-flip transition in the (γ,π^0) channel with subsequent spin-flip transition in the (π^0,π^+) channel. Therefore the spin degrees of freedom in the pion-nuclear interaction significantly affect polarization observables in charged pion photoproduction at backward angles.

Let us return to the study of nuclear structure and operator effects in the polarization observables. In Fig. 7 we show our predictions for the target asymmetry T and the recoil asymmetry P at $\Theta_{c.m.} = 30°$ as a function of the photon energy. As has been shown above, in this angular region these observables are basically insensitive to pion rescattering. Using only the largest S-state components in the three-body wave function or harmonic oscillator S-shell wave functions leads to almost identical results as calculations with the full Faddeev amplitudes (compare dashed and solid curves). The same conclusion holds for the photon asymmetry Σ. This result can be understood in terms of the qualitative discussion in the previous section: At forward direction the transfer momentum is small and, consequently, D-wave contributions which form the $D_M(Q)$ formfactor are small as well. Due to this reason we also found no sensitivity to the $E_{1+}(\Delta)$ multipole in this region.

Thus PWIA with simple S-state wave functions is a good approximation for the Σ, T and P observables in pion photoproduction at small angles. Here the simple relations (16) between the polarization observables on ^{3}He and on the proton are fulfilled. Furthermore, in this region the contribution from the Δ isobar is very important (compare dotted and solid curves in Fig. 7). Therefore, we believe that this is a good kinematical region to study the dominant Δ-isobar properties inside the nuclear medium. Should an experiment find deviations from the simple relations (16) at forward direction, this would indicate

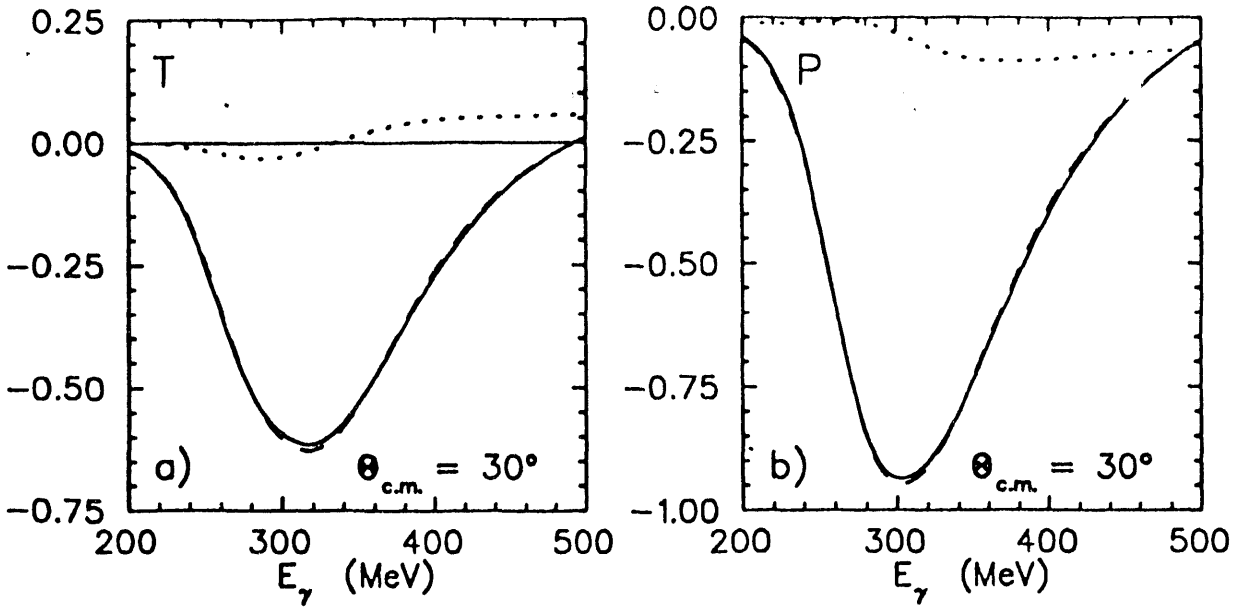

Fig. 7: The observables T (a) and P (b) at 30° as a function of E_γ. Solid (dashed) curves are the calculations with (without) D-state components of the three-body wave function in the coupled-channels framework and with the full production operator. The dotted curves are the calculations with the full wave function but only with Born terms in the production operator.

medium modifications of the delta propagator in the ^{3}He nucleus [23].

Fig. 8 presents the energy dependence for the differential cross section and Σ at $\Theta_{c.m.} = 90°$. Here, as in Fig. 4, we show the sensitivity to the D-wave components and the $E_{1+}(\Delta)$ multipole, but include pion rescattering. The photon asymmetry Σ is less than 0.2 for small photon energies but increases to a maximum value between 0.5 and 0.8 around $E_\gamma = 350 - 400$ MeV. Here the smaller partial waves reduce Σ by up to 30%, leaving a clear signal that should be detectable experimentally. The target and recoil polarizations T and P are sensitive to the D-wave contributions only at higher photon energies around $E_\gamma = 450 - 500$ MeV. However, at these energies the differential cross section is one order of magnitude smaller with values around 10 nb/sr.

The photon asymmetry Σ, on the other hand, is again very sensitive to the presence of the $E_{1+}(\Delta)$ multipole. Above E_γ=350 MeV large differences appear between our computations without and with the $E_{1+}(\Delta)$. The presence of an $E_{1+}(\Delta)$ which is only 5% of the dominant $M_{1+}(\Delta)$ enhances Σ at E_γ=400 MeV by more than a factor of two. The observables T and P are insensitive to the $E_{1+}(\Delta)$ throughout the whole energy region.

7. Conclusion

In summary, we have computed the single polarization observables Σ, T and P for pion photoproduction on the nucleon and the trinucleon. At threshold a measurement of the target and photon asymmetry will allow a complete determination of all the s- and p-wave multipoles. Furthermore, from the unitarity condition of the S-matrix, a measurement of the target asymmetry T (and therefore of ImE_{0+}) gives a direct determination of the πN scattering lengths, that is in the case of neutral pions impossible in pion scattering experiments.

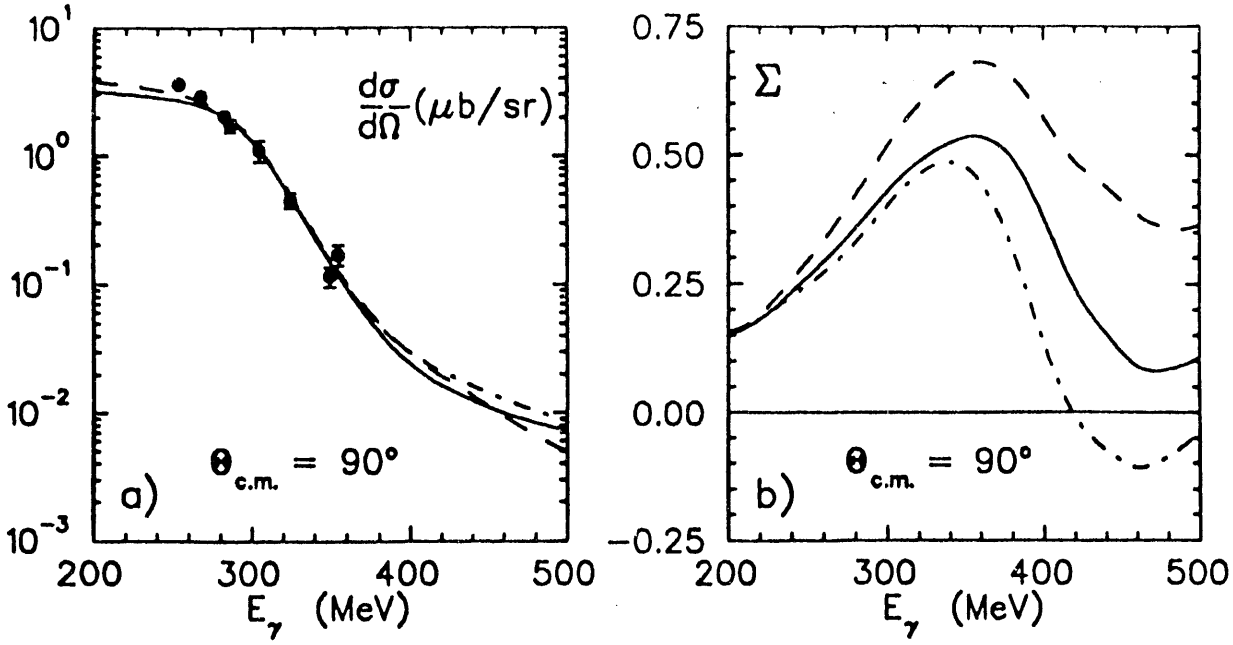

Fig. 8: Differential cross section (a) and photon asymmetry Σ (b) at 90° as a function of E_γ calculated in the coupled-channels framework. The notation of the curves is the same as in Fig. 4. Experimental data for $d\sigma/d\Omega$ are from ref [24].

In the resonance region, the E2(Δ) transition can be determined by measuring the photon asymmetry Σ. For this observable an even bigger sensitivity has been found in the process $^3He(\gamma,\pi^+)^3H$. Our momentum space coupled-channels formalism developed in [4] and used in the present work allows us to consistently describe all experimental data for pion scattering, single charge exchange and pion photoproduction on ^3He at various energies and transfer momenta up to $Q^2 = 8\,fm^{-2}$. We are therefore confident that for a given, well-defined input we can predict polarization observables rather reliably. We find especially the photon asymmetry Σ to be useful to study details in the trinucleon wave function, such as D-state components, as well as the E_{1+} multipole amplitude of the delta. Here an accidental situation in the trinucleon structure will allow a reliable measurements of the E2 excitation of the Δ in the nuclear medium. This would be an ideal supplement to the new starting experimental activities to measure the $E_{1+}(\Delta)$ on the proton directly [15]. Polarized photon beams will become available in the near future at several laboratories; in fact, the LEGS facility [25] at Brookhaven already uses polarized photons in experiments with ^3He [26]. Measuring T should not be difficult as well since several polarized ^3He targets have become available in recent years. On the other hand, obtaining data for P may be more difficult since this involves detection of the recoiling triton which requires a sufficiently large momentum transfer. To advance our knowledge about pion electromagnetic production on few-body systems, measuring polarization observables is a natural step to take.

Acknowledgement

We are very grateful to Prof. A. Bernstein, Dr. R. Davidson and O. Hanstein for their helpful discussions and contributions to this work.

References

[1] R.A. Brandenburg, Y.E. Kim, A. Tubis, Phys. Rev. **C12** (1975) 1368

[2] C. Hajduk, P.U. Sauer, Nucl. Phys. **A369** (1981) 321

[3] J.L. Friar, B.F. Gibson, E.L. Tomusiak, G.L. Payne, Phys. Rev. **C24** (1981) 665

[4] S.S. Kamalov, L. Tiator, C. Bennhold, Few Body Systems **10** (1991) 143

[5] D. Drechsel and L. Tiator, J. Phys. G: Nucl. Part. Phys **18** (1992) 449 and references contained therein.

[6] I.S. Barker, A. Donnachie and J.K.Storrow, Nucl. Phys. **B95** (1975) 347

[7] C.G. Fasano, F. Tabakin and B. Saghai, Phys. Rev. **C46** (1992) 2430

[8] R. Beck et al, Phys. Rev. Lett **65** (1990) 1841

[9] V. Bernard, N. Kaiser, U.-G. Meißner, Nucl. Phys. **B383** (1992) 442

[10] V. Bernard, N. Kaiser, U.-G. Meißner, πN Newsletter No. **7** (1992) 62 and private communication

[11] U.-G. Meißner, Reports on Progress in Physics (1993).

[12] R.M. Davidson, N.C. Mukhopadhyay, R. Wittmann, Phys. Rev. **D43** (1991) 71

[13] A. Bernstein, private communication

[14] J.M. Laget, Nucl. Phys. **A481** (1988) 765

[15] R. Beck, MAMI proposal (private communication)

[16] O. Hanstein, diploma thesis, Mainz (1993).

[17] A.K. Kerman, H. McManus, R. Thaler, Ann. Phys.(NY) **8** (1959) 551

[18] M. Gmitro, J. Kvasil, R. Mach, Phys. Rev. C **31** (1985) 1349

[19] J.M. Källne, et al, Phys. Lett. **B103** (1981) 13

[20] J. Boswell, et al, Nucl. Phys. **A466** (1987) 458

[21] N. d'Hose, Ph.D. Thesis, Saclay 1988.

[22] D. Bachelier, M. Bernas, J.L. Boyard, J.C. Jourdain, P. Radvanyi, Phys. Lett. **B44** (1973) 445

[23] J.M. Koch, E.J. Moniz, Phys. Rev. **C27** (1983) 751

[24] B. Bellinghausen, H.J. Gassen, G. Noeldeke, E. Reese, T. Reichelt, P. Stipp, H.-A. Synal, Nucl. Phys. **A470** (1987) 429

[25] A.M. Sandorfi, IEEE **NS30** (1983) 3083; C.E. Thorn, Nucl. Instrum. Meth. **A285** (1989) 447

[26] G. Adams, D. Tadeschi and M.A. Moinester, BNL(γ^3He) experiment (private communication)

DATE
FILMED
8/25/94
END